TURKISH JOURNAL OF AGRICULTURAL ENGINEERING RESEARCH (TURKAGER)
(Türk Ziraat Mühendisliği Araştırmaları Dergisi)
ISSN:
Research Article (Araştırma Makalesi)
Volume/ Cilt: 1 (2020) Issue/ Sayı :1 (111-130)
https://dergipark.org.tr/tr/pub/turkager

Response Surface Optimization of Convective Air Drying Process in a Hybrid PV/T Solar Dryer

Sampson UZOMA[a] **Nnaemeka NWAKUBA**[b*] **Kelechi ANYAOHA**[c]

[a]*Department of Agricultural and Bio-Environmental Engineering, Imo State Polytechnic, Umuagwo-Ohaji, NIGERIA*

[b]*Department of Agricultural and Bioresources Engineering, School of Engineering & Engineering Technology, Federal University of Technology, P.M.B. 1526 Owerri, NIGERIA*

[c]*Department of Agricultural and Bio-Environmental Engineering, Imo State Polytechnic, Umuagwo-Ohaji, NIGERIA*

(*): Corresponding author. nnaemeka.nwakuba@futo.edu.ng; Tel: +234-803-660-8510

ABSTRACT

The increasing demand for improved techno-economic and efficient drying systems has impelled research on optimization study of solar drying process. This paper discusses the optimization of red pepper slices during drying process in a hybrid photovoltaic-thermal (PV/T) solar dryer using response surface approach. The study was conducted in humid tropical Nigerian environment characterized by intermittent solar irradiance, prompted by humid wind effect from regional water bodies. The effects of varying drying air temperatures (50, 60 and 70˚C), air velocities (1.0, 1.5 and 2.0 m s^{-1}), and sample thicknesses (10, 15, and 20 mm) on the total energy consumption, drying efficiency, %shrinkage, and drying time of pepper samples were investigated using a 3^3-factorial treatment design. The results obtained were built-in and the responses plotted in 3-D surface plots and evaluated statistically to obtain variable relationships. The total and specific energy consumption ranged between 1.31 – 38.9 kWh and 6.92-62.76 kW kg^{-1}, respectively. The percent thermal contribution of the PV module and solar collector at varying air velocities ranged between $0.792\% \leq Q_{pv} \leq 23.53\%$, and $0.518\% \leq Q_{col} \leq 15.37\%$, respectively. The mean system drying efficiency varied between 6.73 - 35.14%, whereas the percentage shrinkage ranged between 56.91 - 73.90%. The drying time varied from 125.5 ± 7 - 205.5 ± 10 mins. At the optimum drying conditions of 70˚C air temperature, 1.88 m/s air velocity and 14.31 mm sample thickness and desirability of 0.903, the total energy consumption, drying efficiency, shrinkage, and drying time were obtained as 4.03 kWh, 20.46%, 67.05% and 183.8 mins, respectively. The predicted models had R^2-values ranging between 0.9228 - 0.9989, which were verified and validated for accuracy using diagnostic plots and percentage error deviations. The results of this study indicate how indispensable some variables and process conditions are to the performance of hybrid PV/T solar dryer.

RESEARCH ARTICLE

Received: 09.04.2020
Accepted: 16.05.2020
Available online: 23.05.2020

Keywords :

- Solar cell,
- Crop drying,
- Energy consumption,
- Efficiency,
- Solar radiation,
- Shrinkage

To cite: Uzoma S, Nwakuba N, Anyaoha K (2020). Response Surface Optimization of Convective Air Drying Process in a Hybrid PV/T Solar Dryer. Turkish Journal of Agricultural Engineering Research (TURKAGER), 1(1): 111-130.

INTRODUCTION

Given the increasing importance of generating clean and cost effective energy for drying of food materials, particularly in developing nations like Nigeria, solar energy has become a promising source of clean energy for drying of plant-based materials due to its marginal cost of operation vis-à-vis cost of fuel (Poonia *et al.,* 2018). This clean, renewable and affordable energy source has been intermittent in its supply `especially in the South-eastern Nigeria, as a result of inter-tropical discontinuity caused by interference of prevalent humid wind from coastal locations and regular rainfall. This in effect, restricts the efficient application of the radiant energy of the sun for drying purposes and had prompted the adoption of a swiftly-developing renewable energy technologies known as solar photovoltaic (PV), which has good future prospects for crop drying. The hybrid photovoltaic/thermal (PV/T) system concurrently generates electric power and heat from incident solar irradiation on the photocell, which are applied to various energy applications such as, domestic heating, agricultural operations etc. Mortezapour *et al.* (2012) reports that photovoltaic cells have the capability of converting only 20% and 80% of the absorbed solar flux to electric energy and to heat, respectively. This raises the temperature of the photovoltaic cell, thereby reducing the electrical efficiency conversion of the system. In a bid to circumvent this challenge, necessitates the advent of hybrid PV/T technology.

Convective drying of food materials is characterized by low thermal conductivity which requires large quantity of energy due to insufficient and inefficient intra-cellular heat transfer (Nwakuba *et al.,* 2018). This is mostly significant in an environment where the heat-carrying capacity of the air stream is grossly small as a result of increased ambient relative humidity. Optimizing the operational conditions of convective drying process amongst its importance, reduces the overall energy cost for crop drying, improves efficiency of the dryer, as well as improved dried product quality.

Pepper (*Genus Capsicum*) is an essential fruit vegetable, given its monetary benefits as well as the dietary and health advantages. It is rich in nutrients - Vitamins A, C, K, and B6, calcium, iron, zinc, and fiber. Pepper is mostly used for the purposes of culinary and seasonings and considers to be one of the most valued spices in Nigerian delicacies used either in fresh, dried or powdery form. In Nigeria, pepper has high demand because of its pungency and good taste, and can easily be dried, ground and packaged for export. Its use in Nigeria represents about 40 percent of the total vegetable consumption in a day (Sanusi and Ayinde, 2013). The dried Savannah region of Nigeria has high potential for pepper production. Huge postharvest losses are usually encountered during commercial scale production because of the commonly used open sun drying practice. Given its high moisture content (82 – 88% w.b), labour intensive and time-consuming drying operation, a suitable dryer is required for large-scale quality-dried pepper product. This would benefit Nigerian farmers economically and help fulfill their national and international requirements.

Response surface optimization offers data for optimizing or evaluating numerous responses, and simultaneously produce statistical-based accurate mathematical

relationships used for graphical analysis of the method studied. These models illustrate the influence of input parameters on responses, estimate their interaction effects and denote the combined effect of the input parameters in a response in graphic form. This technique, according to Erbay and Icer (2009) allows the researcher to make effectual survey of a system or process. Different techniques of optimization exist such as, the generally used graphical technique, the improved graph method, the desirability function, and the stretched surface method (Corzo *et al.*, 2008). Response surface optimization has been often adopted in drying of food materials (Corzo *et al.*, 2008; Erbay and Icer, 2009; Han *et al.,* 2010; Kumar *et al.*, 2011; Abano *et al.,* 2014; Nwakuba, 2019).

This study considers adopting the response surface technique for obtaining the best drying settings for convective air drying of red pepper slices using a PV/T solar dryer in a location prone to inter-tropical discontinuity. There are currently, limited published literature on the optimal control variables for cost and energy effective drying of fruit vegetables in humid tropical zones using solar photovoltaic technology. Therefore, the main objective of this paper therefore to optimize the parameters for convective air drying of sliced red pepper by adopting the desirability index approach, which describes the technique of response surface in determining the optimal total energy consumption, drying efficiency, drying time and percent shrinkage within the range of varying levels of control variables (drying air temperature, air velocity, and sample thickness) during red pepper drying process. However, this would facilitate the design of experiments by eliminating labourious experimental runs without compromising vital technical information, as well as promote selection of best drying conditions that would require little drying energy and carbon emission and increase dryer cost effectiveness with very minor deleterious effect on the dried food product. The optimization result therefore, was studied by using a 3x3 factorial design layout of Central Composite Design (CCD) of Design-Expert (11.0) Statistical tool.

Achieving substantial energy reserves during convective hot air drying process of fruit vegetables, apprehensions on drying economics and effects on food security/supply, ecological emissions, and provision of optimal total energy for drying, temperature of the drying air, velocity of the drying air stream, sample thickness, drying efficiency, percentage shrinkage, and drying time most appropriate for red pepper justifies this work. This paper would present empirical mathematical relations that predict energy consumption of hybrid PV/T solar dryer as well as other response variables and process conditions for red pepper slices, which are indispensable in the design of energy-efficient and cost-effective hybrid PV/T solar dryers for fruit vegetables.

MATERIAL and METHODS

Experimental Procedure

Drying experiments were conducted at Imo State Polytechnic, Umuagwo-Ohaji, Nigeria, between 3rd - 11th September 2019. This period of the year in Nigeria is known for high rainfall intensity and ambient relative humidity, as well as low/intermittent sunshine. It also coincides with the time of harvest for the majority of farm produce in this region, which requires immediate drying for better and prolonged storage. The study made use of a hybrid convective PV/T solar dryer (Fig. 1), primed with arduino microprocessor to control and measure the temperature of drying air,

velocity of drying air, and air relative humidity in the drying chamber, solar collector unit and the surrounding. The dryer was placed in an open area and switched on to attain steady-state condition. The solar cell (PV module) is of silicon mono-crystalline type with specification: 1.3 x 0.65 m^2. It has a thickness of 0.0003 m and absorptivity of 0.85; whereas the solar collector (Fig. 1, No. 7) with a rectangular configuration of 0.1 x 0.65 x 0.3 m^3 has a 0.01 m absorber plate, 0.04 m thick plain glass, and a duct width of 1.5 m mounted on a frame support.

Non-pretreated fresh red pepper samples purchased from Relief market in Owerri metropolis were selected based on mass, viability and colour. Mean sample initial moisture content of 81.9% wet basis (w.b) was obtained using oven method at 105°C for 24 hours (Nwakuba *et al.,* 2019). A batch of 0.5kg of the sliced samples was measured and selected using a digital weighing balance and a stainless-steel knife (Fig. 2). Experiments were carried out with three drying air temperatures (50, 60 and 70°C), air velocities (1.0, 1.5 and 2.0 m/s) and sample sliced thicknesses (10, 15 and 20 mm). It is worthy of note to point out that the selected air velocity range corresponds to the maximum and minimum airflow rates obtained in the study area during harvesting season; whereas the range of sample thickness reflects the sizes of studied red pepper variety available in the local vegetable market. However, weight sensors connected to the drying racks recorded moisture losses per 10 minutes interval and transfer data to a personal computer via the arduino processor control panel. A pyranometer was used to measure the amount of incident radiation on the solar collector. The total energy consumption (from solar cells and solar collector) and drying time for each batch were recorded. The experiment was ended when the sample moisture loss reached the desired final moisture content of 10% w.b (Tiwari, 2012; Uzoma *et al.,* 2019).

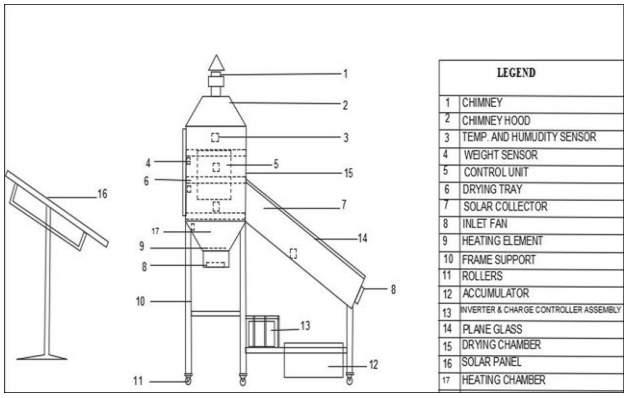

Figure 1. 2-D diagram of the hybrid PV/T solar dryer

Figure 2. Thin layer sliced red pepper samples.

Experimental Design and Response Surface Analysis

The drying experiment was formulated in a factorial treatment design of the central composite design (CCD) tool of Design Expert Statistical Software (version 11.0), in a randomized form so as to lessen the unexplainable effects in the observed response variables. Three independent input variables: air temperature (T), air velocity (V), and sample slice thickness (S) at three levels each, for four response variables, Y_r (total energy consumption, drying efficiency, drying time and shrinkage) were formed. The relative contributions of each of the independent variables to the response variables (Y_r) were determined. A 3^3 layout of CCD RSM for the drying experiments is shown in

Table 1. In order to optimize the drying conditions of the hybrid solar-electric dryer, Eq. (1) was applied to describe the linear, interaction and curvature effects of the response variables expressed as:

$$Y_r = \beta_0 + \beta_1 T + \beta_2 V + \beta_3 S + \beta_4 TV + \beta_5 TS + \beta_6 VS + \beta_7 T^2 + \beta_8 V^2 + \beta_9 S^2 \quad (1)$$

Where: β_0 represents the model intercept; β_1, β_2, β_3, …, β_9 are coefficients of the regression model; $\beta_1 T$, $\beta_2 V$, and $\beta_3 S$ are the linear effects; $\beta_4 TV$, $\beta_5 TS$ and $\beta_6 VS$ are the model interaction effects; $\beta_7 T^2$, $\beta_8 V^2$ and $\beta_9 S^3$ represent the quadratic effects.

However, Eq. (1) was arranged in line with the RSM quadratic model obtained from this study, which mathematically describes the relationship between the input drying factors.

Table 1. Experimental layout of input factors and Levels of the randomized factorial treatment design

Input variables	Coded symbol	Levels	
		Actual	Coded
Air temperature (°C)	T	50	-1
		60	0
		70	1
Air velocity (ms^{-1})	V	1.0	-1
		1.5	0
		2.0	1
Sample thickness (mm)	S	10	-1
		15	0
		20	1

The desirability index, D(x) which adopts the method of multivariate responses of numerical optimization of the drying process is given by Eq. (2) as (Kumar *et al.*, 2011; Nwakuba, 2019):

$$Y_r = \left[Y_{r1} . Y_{r2} . Y_{r3,} \ldots, Y_{rn} \right]^{-n} \quad (2)$$

Where: n is the total number of responses = 4; D(x) ranges between 0 and 1, donating the lowest and highest desirable coded levels, respectively.

Objective function

D(x) shows the extent to which the experimental response variables are closely matched or compactible to a given level of input parameter. In this study, the optimization goals for the input parameters are taken within the design limit of the input values, whereas the response parameters considered minimum energy consumption, maximum drying efficiency and minimum drying time and percent shrinkage of the dried products (Table 2). The high value of D(x) which indicates the most apt functions for the drying process of pepper gives the system optimal solution (Nwakuba, 2019). The optimum values of the experimental factors were obtained from the total energy consumption, drying efficiency and shrinkage variables which maximize D(x). Analysis of variance (ANOVA) was adopted to estimate the significance of the model variables at 5% probability level ($P < 0.05$), as well as the

influence of the input parameters on the response variables. It also validates the accuracy of the prediction models, whereas degree of freedom (df), mean square (ms), sum of squares (ss), F and P-values check the model efficiency (Freedman *et al.*, 2007). Least significant differences in the experimental variables were checked using the Fisher's test.

The accuracy of prediction of the response variables was verified using Diagnostic plots, such as the normal probability plots of the residual response parameters, plots of predicted versus experimental response parameters, Box-cox plot (natural log of the residual sum of squares, Ln residual SS), and coefficient of determination (R^2); meanwhile the model adequacies were obtained from the adjusted-R^2 and coefficient of variation (CV). It is pertinent to state that the reliability of the developed models to predict experimental data is a function of the Lambda value for each response variable.

Table 2. Criteria and goals for numerical optimization

Input/Response variables	Goal	Lower limit		Upper limit		Importance
		Actual	Coded	Actual	Coded	
Temperature (°C)	in range	50	-1	70	1	3
Air velocity (ms^{-1})	in range	1.0	-1	1.5	1	3
Sample thickness (mm)	in range	10	-1	20	1	3
Total energy consumption (kJ)	minimize	-	-	-	-	3
Drying efficiency (%)	maximize	-	-	-	-	3
Shrinkage (%)	Minimize	-	-	-	-	3
Drying time (mins.)	minimize	-	-	-	-	3

Theoretical Calculations

Energy analysis

The total energy flow of the hybrid system (Q_t) is the sum of the total irradiation on the solar collector and PV during the sunlight and the thermal/electrical energy generated is expressed as:

$$Q_t = Q_{col} + Q_e + Q_{pv} \quad (3)$$

Where: Q_{col}, Q_e, Q_{pv} = total radiation on solar collector, thermal energy from resistance wire, and photovoltaic energy (kWh), respectively.

According to Duffie and Beckman (2006), Q_{col} is given by:

$$Q_{col} = A_c F_R[(\alpha_g \tau_g) - U_o (T_c - T_a)] \quad (4)$$

The overall thermal loss (U_o W/m^2) from the solar collector (top, bottom, and sides) is given by Ndukwu *et al.* (2020a) as:

$$U_o = U_t + U_b + U_s \quad (5)$$

The useful thermal energy from the electric heater unit is expressed as:

$$Q_{pv} = \eta_{pv} \tau_g^2 \beta I_g A_c \quad (7)$$

Where: F_R = heat removal factor; A_c = solar collector area (m^2); $\alpha_g\tau_g$ = effective transmittance-absorbance of glass (0.06x0.84); U_o = overall heat thermal loss (W/m^2); T_c and T_a = solar collector temperature and ambient air temperature, respectively (^oC); $\dot{M}$ = mass flow rate of air (kg/s); C_p = specific heat capacity of air (J/kg;); T_o and T_i = outlet and inlet air temperatures of the heater (^oC), respectively; η_{pv} = PV efficiency (0.116%); $\tau_g^{\ 2}$ = transitivity of glass (0.84); β = fill factor (0.708); I_g = incident solar flux (W/m^2); hp is the heater rated power (W), a_h = heater area (m^2), l_h = heater length (m), t = drying time (s); U_t, U_b, and U_s = thermal loss from top, bottom, and sides, respectively.

Since drying was done during inclement weather condition, the total energy consumption during drying process at varying air temperatures and air velocities is expressed considered Eq. (3).

The specific energy consumption for drying a kg sample mass is expressed as (Afolabi *et al.*, 2014; Nwakuba *et al.,* 2018):

$$Q_s = \frac{Q_t}{M_w} \tag{8a}$$

Where: $M_w = M_t - M_{t+1}$ (8b)

Q_s = specific energy consumption ($kWhkg^{-1}$, M_w = mass of water removed from the sample (kg), M_t = mass at time t and M_{t+1} is the next mass after M_t.

Drying efficiency

The drying efficiency of a hybrid PV/T solar dryer (η_d), is given by (Uzoma *et al.,* 2019; Ndukwu *et al.,* 2020b):

$$\eta_d = \frac{M_m.L}{Q_t} \tag{9}$$

Where: M_m = quantity of moisture expelled (kg), L = latent heat of vaporization of moisture (kJ/kg).

Shrinkage analysis

The percent shrinkage of a product is one of the vital parameters assessing the quality of dried products, as it determines the rehydration rate of the dried product. Shrinkage indicates the relative change in the sample thickness as a result of moisture removal during drying process. The shrinkage percentage, S was obtained by determining the initial and final sizes of the pepper slices using the method of liquid displacement (Hafezi *et al.*, 2015). For each experimental treatment, three samples were selected in random, and percent shrinkage of the pepper samples was obtained as (Dianda *et al.,* 2015; Hafezi *et al.*, 2015):

$$S_h = \left(1 - \frac{V_i}{V_d}\right) \times 100\% \tag{10}$$

Where: S_h = Shrinkage (%), V_i and V_d = initial and dried volumes of the pepper slices, respectively (m^3).

RESULTS and DISCUSSION

The layout of the experimental factors (with 20 runs and 19 degrees of freedom) of the drying parameters and responses are as presented in Table 3. The coefficients of the input parameters and their interactions, as well as the resulting quadratic prediction functions of the response variables were obtained from the experimental data of Table 2.

Table 3. Central composite design of the experimental input and response variables

Run No.	Input Variables			Response Variables			
	Temperature, T (oC)	Air velocity, V (ms-1)	Sample thickness, S (mm)	Total energy, Et (kWh)	Drying efficiency, η_d (%)	Shrinkage, Sh (%)	Drying time, Td (mins)
1	50.00	1.00	10.00	16.54	7.12	56.91	197.50
2	70.00	1.00	10.00	9.38	12.81	62.71	150.00
3	50.00	2.00	10.00	10.54	15.45	68.89	179.50
4	70.00	2.00	10.00	1.31	18.38	61.18	140.00
5	50.00	1.00	20.00	35.72	20.27	66.24	150.00
6	70.00	1.00	20.00	9.23	29.94	73.92	125.50
7	50.00	2.00	20.00	30.67	29.75	72.99	201.50
8	70.00	2.00	20.00	2.28	33.12	70.14	150.00
9	43.18	1.50	15.00	38.91	12.41	57.55	144.50
10	76.82	1.50	15.00	5.86	25.86	60.88	150.50
11	60.00	0.66	15.00	15.82	9.22	68.72	205.00
12	60.00	2.34	15.00	6.22	20.86	72.17	158.50
13	60.00	1.50	6.59	4.31	16.51	61.12	193.50
14	60.00	1.50	23.41	19.43	30.41	74.87	196.50
15	60.00	1.50	15.00	9.11	20.82	68.23	194.50
16	60.00	1.50	15.00	8.49	20.82	67.16	190.00
17	60.00	1.50	15.00	9.16	20.82	65.19	194.50
18	60.00	1.50	15.00	9.33	20.82	70.01	192.00
19	60.00	1.50	15.00	8.82	20.82	65.87	190.50
20	60.00	1.50	15.00	9.37	20.82	67.13	191.50

The results of the ambient air condition during the drying process is presented in Fig. 3. The mean heat outflow and thermal/electrical energy developed by the solar collector and PV module respectively were dependent upon the solar radiation intensity, which varies with time of the day. Reduction in solar irradiation due to cloud change reduced the ambient air temperature and negatively affects the performance efficiency of the dryer. As hourly time increased, the amount of solar radiation increased to a maximum of 714.38 Wm^{-2} at 1:00pm with ambient air temperature and began to decrease. This proportional increase in air temperature raised the pressure of water vapour in the air, lowered the relative humidity of air, and thereby enhanced the specific moisture extraction rate. However, the ambient air had the highest relative humidity (85.1%) at 10am and decreased as solar radiation and hourly time increased, which resulted in gross reduction in the enthalpy of the solar collector air temperature. Drying operation was done at a mean ambient air temperature, relative humidity, and solar radiation of 27.24^{o}C, 62.6%, and 518.2 Wm^{-2}, respectively.

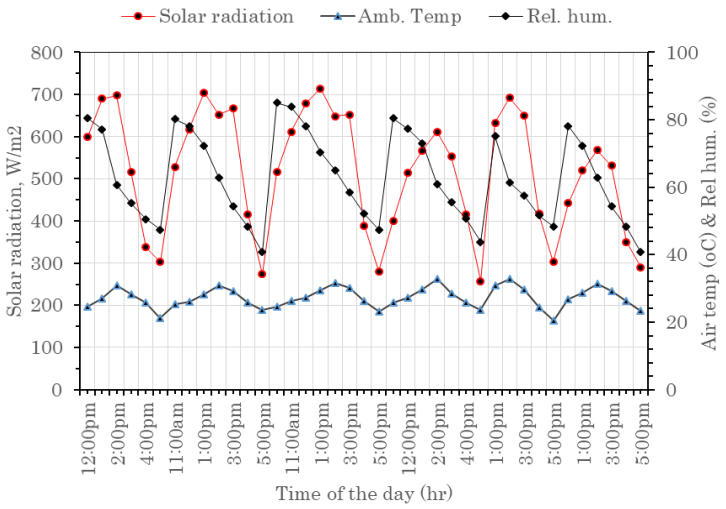

Figure 3. Mean ambient air condition during drying process

Thermal energy contribution of solar collector and solar cell

The percent useful thermal energy input of the solar collector and solar cell to the hybrid system is shown in Table 4. Since the PV module converts incident solar flux to electric heat output (at negligible loss in surface temperature of solar cell), the sum of Eqs. (6) and (7) were subtracted from the total energy flow of the hybrid system (Eq. 1) to obtain the solar collector energy contribution. The total heat energy contribution of the solar cell during the sunshine periods ranged between $0.792\% \leq Q_{pv} \leq 23.53\%$, whereas the solar collector contribution varied from $0.518\% \leq Q_{col} \leq 15.37\%$ at increasing air velocity. Increasing the velocity of drying air enhanced the rate of convectional heat transfer to the drying chamber, thus higher % heat contribution for drying. The lower percent contribution of the solar collector can be attributed to low mean ambient air temperature of 27.24^{o}C, which is inadequate for moisture removal from high moisture product like red pepper. Operating the PV/T hybrid dryer at an air velocity of 2.0ms^{-1} would undoubtably reduce its energy consumption, improve drying efficiency, and drying rate.

Table 4. Percent energy contribution of solar collector and solar cell

Air velocity (ms^{-1})	Percent energy contribution (%)	
	Solar cell	Solar collector
1.0	0.792	0.518
1.5	12.73	7.94
2.0	23.53	15.37

Variance Analysis of Drying Variables and Reponses

Energy consumption

The effect of interaction of the drying parameters on the total and specific energy consumption are illustrated in Figs. 4 and 5. At constant sample thickness, increasing the drying air temperature and air velocity reduced the total and specific energy consumption of the drying process. This is because of the increase in the rate of heat and mass transfer in the sample product and reduction in the water vapour pressure which resulted in less resistance moisture diffusion and evaporation, thereby reducing the drying time hence, gross reduction in the total and specific energy consumption.

Similar observations were reported by Darvishi *et al.* (2013), Minaei *et al.* (2014), Hafezi *et al.* (2015).

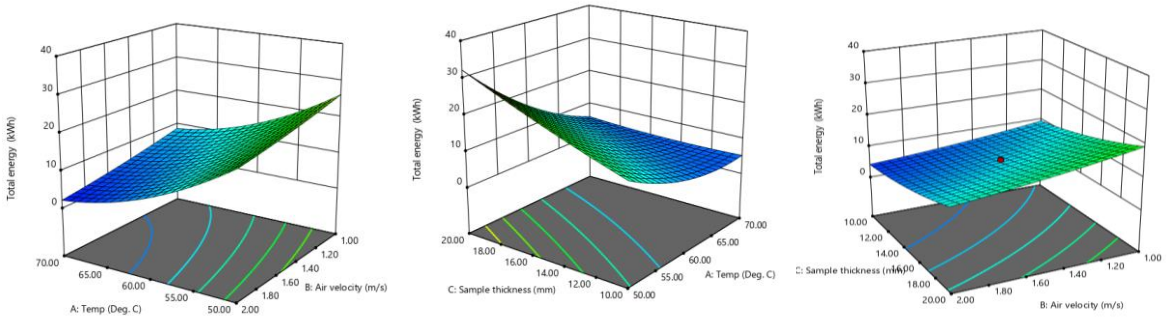

(a) **(b)** **(c)**

Figure 4. Response surface plot interaction between: (a) drying air temperature and air velocity, (b) drying air temperature and sample slice thickness, (c) air velocity and sample thickness, on the total energy consumption

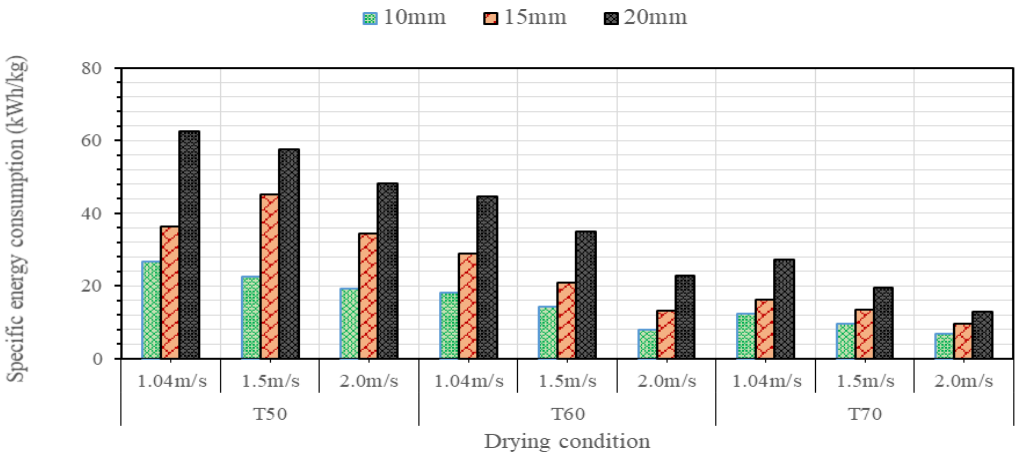

Figure 5. Influence of the drying variables on the specific energy consumption of red pepper

Less total and specific energy were consumed by the pepper samples at constant air velocity by increasing the drying air temperature at a corresponding decrease in the sample thickness. This could probably be as a result of increased moisture diffusion rate and reduce distance of capillary transport in the sample product, which decreased the energy consumption through reduction in drying time. Nwakuba (2019) reported a similar observation in drying of tomato slices using a hybrid solar-electric dryer. Increasing the air velocity at constant air temperature increases the rate of heat transfer to and from the product, hence reduction in energy consumption. However, the total and specific energy consumption ranged from 1.31 – 38.9 kWh and 6.92 – 62.76 kW/kg, respectively. The minimum total energy consumption of 2.28 kWh was obtained at the highest values of drying air temperature (70^{o}C) and air velocity (2.0 m/s), and lowest sample thickness (10 mm), whereas the minimum and specific energy consumption of 6.92 kWh/kg was obtained at 70^{o}C air temperature, 2.0m/s air velocity and 10mm sample thickness.

Eq. (11) expresses the 2nd order quadratic model of the total energy consumption for drying a batch of the red pepper sample at varying drying parameters in coded terms:

$$E_t = 9.03 - 8.85T - 2.96V + 4.67S + 4.21T^2 + 0.63V^2 + 0.94S^2 - 0.27TV - 5.05TS + 0.049VS \quad [R^2 = 0.9989] \quad (11)$$

The positive and negative model parametric coefficients indicate synergistic and antagonistic influence on the total energy consumption of red pepper, respectively. From Eq. (11), air velocity with the highest negative coefficient of -2.96 was the most ineffective parameter for reduction of energy consumption, whereas the most effective parameter for energy reduction was sample thickness, which had the highest positive coefficient of 4.67. The normal probability plot of the total energy consumption residuals also validated the energy model (Figs. 6a & b). The clustering of the plotted data on the fitted line indicates equality between the values of predicted and experimental total energy consumption, which also confirms that the degree regularity and experimental outliers in the analyzed data had no negative effect on the resulting model. Validation of the prediction accuracy of the developed energy model was done by the Box-Cox graph, after transformation of experimental data through power equations (Ahmad *et al.,* 2015). Fig 6c illustrates that the Lambda value, which denotes the power given to the values of the response variable was 0.92, which later had a current Lambda value of 1.0 after power transformation. The diagnostic plots in Fig. 6 generally signify that the energy model completely captures the anticipations of ANOVA.

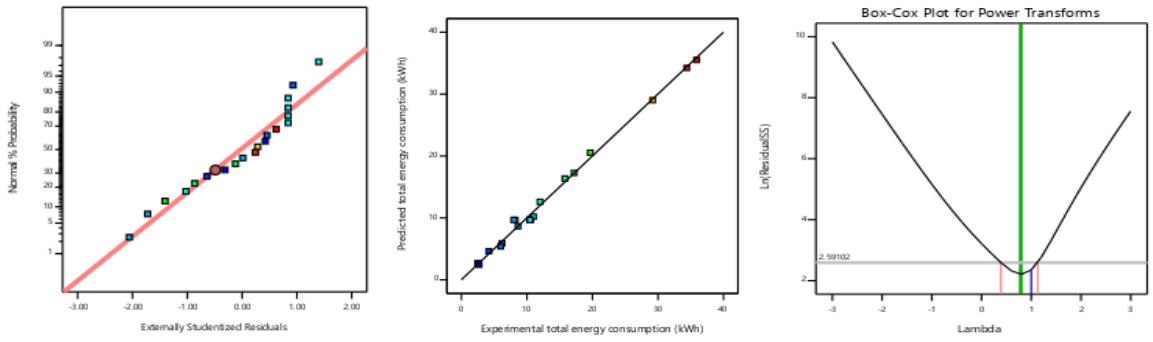

(a) **(b)** **(c)**

Figure 6. (a) Normal probability plot of the total energy consumption residuals; (b) Predicted versus experimental total energy consumption of red pepper; (c) Box-Cox plot for power transformation

The analysis of variance conducted for the total energy consumption depicts that the model F-value, which determines the variance of total energy consumption data about the mean indicates that the model is significant. From statistics perspective, the "Prob. > F" values endorse the predicted energy relationship. P-values less than 5% show significant model variables. In this case, T, V, S, T^2, V^2, S^2, TS are significant model variables; whereas values > 10% indicate non-significant model variables (TV and VS). The "lack of Fit F-value" of 2.96 is an indication that lack of fit is not significant in relation to the "pure error" and proper fitting of model to the experimental data points. There is a 12.93% chance that "Lack of Fit F-value" this large can be attributable to noise. Insignificant lack of fit is a sign of good model fit (Kumar *et al,* 2011; Nwakuba, 2019). The model's R^2-value of 0.9989 shows proper model fit, and strong correlation of the values of the predicted and experimental energy consumption, as well as accounted for a larger proportion of the variations in the experiment. In other words, the experimental data were adequately described by

the model, which closely predicted the total energy consumption as indicated by a low CV-value (3.60%) less than 10% (Abano *et al.,* 2014, Nwakuba *et al.,* 2018). The predicted R^2-value of 0.9930 strong agrees with the adjusted R^2 of 0.9979. "Adeq. Precision" tests the proportion of experimental inputs and noise. A proportion > 4 is desirable (Kumar *et al.,* 2011). A ratio of 101.802 indicates an adequate signal, thus the model to move around the design environment.

Drying efficiency (η_d)

Fig. 7 depicts the influence of drying variables on the system drying efficiency, which increases with increasing drying variables. This is probably as a result of high temperature gradient between the drying air and the product, as well as increased heat and mass transfer rates, heat removal factor of the solar absorber plate and electric heater which increase the total useful heat of the drying air as well as improve the product drying rate, thus enhancing the drying efficiency (Lopez-Vidana *et al.,* 2013; Reyes *et al.,* 2014; Uzoma e*t al.,* 2019). Decreasing the sample thickness at constant (reduced) drying air temperature and air velocity reduced the average drying efficiency, because of decline in the heat transfer rate and intra-particle moisture diffusion. Since drying efficiency, η_d is the ratio of total energy consumption for sample moisture evaporation to the quantity of energy supplied to the system, it generally implies that drying larger sample thickness at constant drying air temperature and air velocity consumes more thermal energy per kW energy supplied, thus increase in η_d. The mean system drying efficiency ranged between $6.73\% \leq \eta_d \leq 35.14\%$. This result corroborates with the reports of Boughali *et al.* (2009) and Beigi (2016) who obtained drying efficiency values between 2.50 – 54.37%.

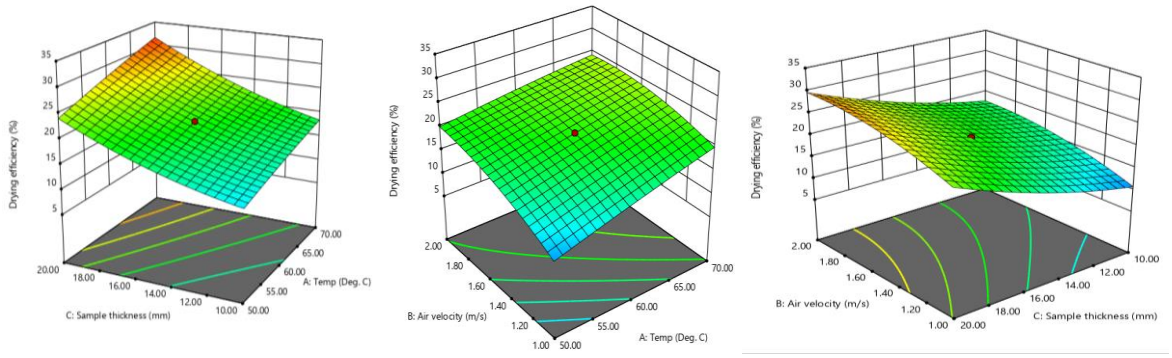

(a) **(b)** **(c)**

Figure 7. Response surface plot interaction between: (a) drying air temperature and air velocity, (b) drying air temperature and sample slice thickness, (c) air velocity and sample thickness, on the drying efficiency

From the analysis of variance (ANOVA) for drying efficiency (η_d), the model F-value indicates that the model is significant. The model terms with P-values < 0.0001 indicate that only T, V, S, V^2, S^2 and TV are significant and vital model parameters. The model had non-significant lack of fit, which is good for the model to fit. There is a 99.73% chance that "lack of fit F-value" this large is attributable to noise. The high R^2 of 0.9228 indicated strong correlation between model parameters. The RSM has the capability to explain greater proportion of the variability in the observed data. The predicted R^2 of 0.9930 of the model is adequately close to the Adj. R^2 of 0.9979. "Adeq. Precision" of 49.166 indicates a satisfactory proportion of experimental and noise. The

model can be applied for optimizing the drying efficiency of red pepper in a PV/T solar dryer.

The diagnostic plots (Fig. 8) from the experimental data were used to check and estimate the model adequacy. The results depict that the proximity of the observed data to the fitting line shows an appreciable relationship between the predicted and observed data. Box-Cox plot validated the accuracy of prediction of the model by power transform of η_d to Lambda value = 1.00, with random residual dispersion between -3 to 3 in the domain. The Lambda value, which indicates the power given to the response variable, which was 0.86 after transformation had a Lambda value = 1. The response variable raised to the power of 1 remains its value, that is $(\eta_d)^1 = \eta_d$. Thus, the developed relation has the capability to accurately forecast the observed data. The expression for η_d in coded terms is expressed in Eq. (12) as:

$$\eta_d = 20.46 + 3.25T + 2.41V + 1.19S - 0.13T^2 - 1.68V^2 + 1.46S^2 - 1.04TV + 0.59TS - 0.26VS \quad [R^2 = 0.9228] \tag{12}$$

From Eq. (12), drying air temperature with the highest positive coefficient (3.25) was most effective in increasing the drying efficiency.

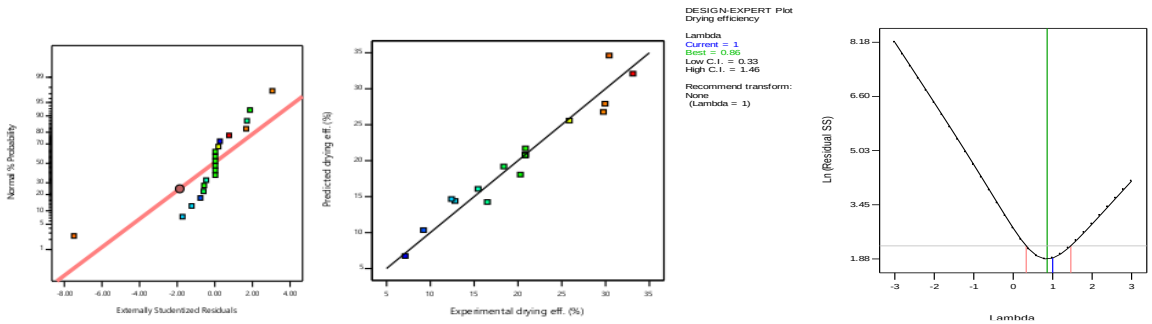

(a) **(b)** **(c)**

Figure 8. (a) Normal probability plot of drying efficiency residuals; (b) Predicted versus experimental drying efficien of red pepper; (c) Box-Cox plot for power transformation

Shrinkage

The percentage shrinkage, S_h of the dried red pepper samples at varying drying parameters, calculated from Eq. (10) is shown in Fig. 9. It was observed that sample shrinkage decreased with decreasing sample thickness, drying air temperature and air velocity. In other words, drying air temperature and air velocity have noticeable effects are proportional to shrinkage changes at given sample thickness. Fig. 9 could be attributed to more loss of water and matrix heating in thicker samples at higher drying air temperatures and air velocity, which cause noticeable stresses in the intra-cellular structure of food material, resulting in decreased dimension and shape change (Hafezi *et al.,* 2015).

The percentage sample shrinkage, S_h ranged between $56.91\% \leq S_h \leq 73.90\%$. The ANOVA obtained showed that the model is significant (F-value = 26.51) at $P > 0.01$. The model terms are significant at $P < 0.0001$, except V^2, TV, TS and VS. The model has lack of fit F-value of 0.41 which is not significant, implying that 82.58% chance that "Lack of Fit F-value" this large is attributable to noise. Non-significant lack of fit is good, hence the mode would fit the experimental data. The coefficient of

determination, R^2 of 0.9598 also indicated proper fitting of the model and its ability to explain 95.98% of the shrinkage changes in the dried samples. The "Pred. R^2" of 0.9174 and "Ad. R^2" of 0.9236 are in close agreement. The measure of the signal to noise ratio > 4 is desirable, and is given by "Adeq. Precision" of 18.08, indicating adequate signal to noise ratio, hence suitability of the model to optimize shrinkage response. The model fitness was checked by analyzing the residual plots shown in Fig. 10 (a - c). The pattern of data distribution was determined by plotting the normal % probability against studentized residual. The normal distribution of data in the model response was also indicated by the considerable clustering of the residuals on the straight line, thus accurate prediction of the experimental data. Lambda value of 1 was suggested by the Box-Cox graph after transformation for percent shrinkage. A 2nd-order quadratic model is completely suitable for prediction of percentage shrinkage from experimental data as expressed in Eq. (13). Sample thickness, with the highest negative coefficient of -1.12 was the most effective variable to reduce shrinkage, followed by drying air temperature.

$$S_h = 67 - 1.95T + 1.41V - 1.12S - 2.59T^2 + 1.38V^2 + 0.51S^2 - 3.00TV + 0.84TS - 0.93VS \quad [R^2 = 0.9598] \tag{13}$$

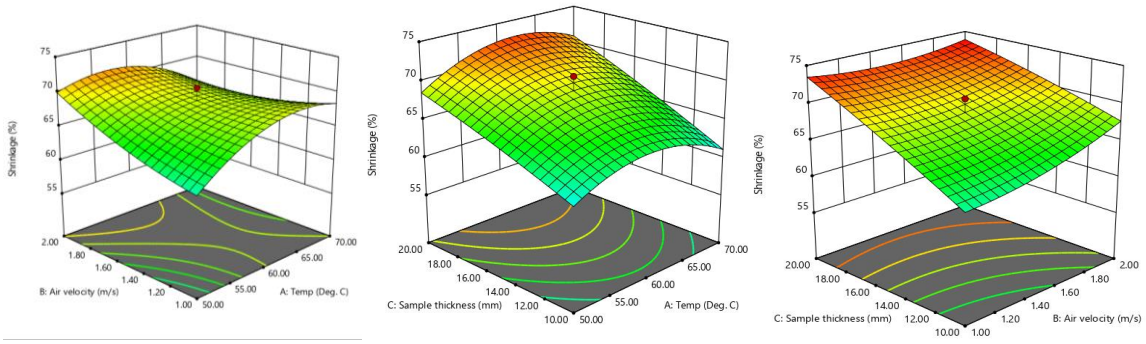

(a) **(b)** **(c)**

Figure 9. Response surface plot interaction between: (a) drying air temperature and air velocity, (b) drying air temperature and sample slice thickness, (c) air velocity and sample thickness, on the percent shrinkage

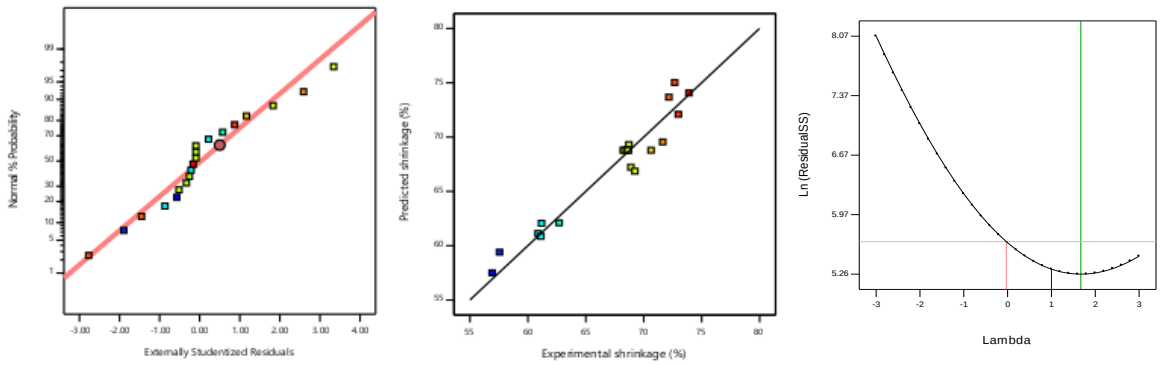

(a) **(b)** **(c)**

Figure 10. (a) Normal probability plot of shrinkage residuals; (b) Predicted versus experimental total energy consumption of red pepper; (c) Box-Cox plot for power transformation

Drying time, T_d

The predicted drying time was observed to decrease with increasing drying air temperature at decreasing sample thickness and air velocity (Fig. 11). Drying rate was

increased as temperature of drying air increased, hence reduction in T_d. Large capillary distance of moisture diffusion as well as air turbulence above a critical level (which causes turbulence at dryer plenum), reduces drying rate, thus reduction in drying time (Boughali *et al.,* 2009). Other researchers like Darvishi *et al.* (2013), Azadbakht *et al.* (2017) reported similar observations. Drying air temperature and sample thickness were highly significant at 1% and 5% levels of probability. Minimum T_d occurred at 70°C air temperature, 1.5 m/s air velocity and 10mm sample thickness. Drying air temperature was observed to have more significant effect on the drying time than air velocity at given sample thickness, as a result of greater quantity of energy consumption was used to increasing the drying chamber air temperature and relative humidity above ambient level in order to raise drying capacity of the convective air. The drying time of red pepper varied between $125.5 \pm 7 \leq T_d \leq 205.5 \pm 10$ mins.

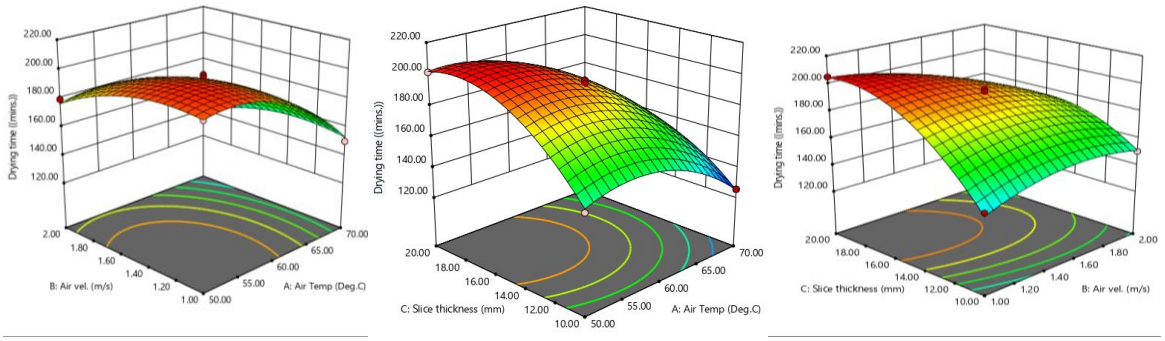

(a) **(b)** **(c)**

Figure 11. Response surface plot interaction between: (a) drying air temperature and air velocity, (b) drying air temperature and sample slice thickness, (c) air velocity and sample thickness, on the predicted drying time

The ANOVA for response quadratic model of shrinkage showed that the T_d-predicted model is significant (F-value = 133.14) at Prob. > F less than 0.05. The model terms as well as their interaction effects are significant ($P < 0.005$) except V, V^2, and TV terms. The "Lack Fit F-value" of 2.44 indicates that the Lack of Fit is not significant ($P > 0.005$) with respect to pure error. There is a 20.46% chance that "Lack of Fit F-value" this large is attributable to noise to noise. A non-significant "Lack fit F-value" is good for model fitting. The "Pred. R^2" = 0.9467 shows good relationship with the "Adj. R^2" = 0.9842. Adequate precision > 4.0 is desirable and indicates adequate proportion of experimental and noise. The coefficient of determination, R^2 = 0.9942 (Eq. 14) confirms strong correlation between drying time and the drying variables. The suitability of the T_d-model was validated with the normal % probability plot, and the plot of predicted versus experimental drying time (Figs. 12a and b). The results show that the experimental data lined-up along the model fitting line, indicating that the predicted and experimental T_d data are equal.

The prediction accuracy of the model was checked by the Box-Cox plot (Fig. 11c) after power transform of Lambda value of 1 for T_d. It is evident that the quadratic model has the capability to forecast very accurately the experimental data and explains 99.42% changes in the drying time of red pepper slices in a hybrid PV/T crop dryer. The resulting relationship (Eq. 14) after Lambda power transform = 1 is expressed thus:

$$T_d = 193.80 - 12.17T - 19.56V + 18.06S - 17.46T^2 - 9.59V^2 - 19.59S^2 + 2.0TV - 6.75TS - 13.13VS \ [R^2 = 0.9942] \quad (14)$$

It was observed that drying air temperature and sample thickness have antagonistic effect to T_d; reduction in the sample thickness decreases T_d. Since sample thickness, S is the only variable with positive coefficient (18.06), was the most effective T_d-reduction variable, whereas drying air temperature, T with the highest negative coefficients of -12.17 was the most ineffective variable to T_d-reduction.

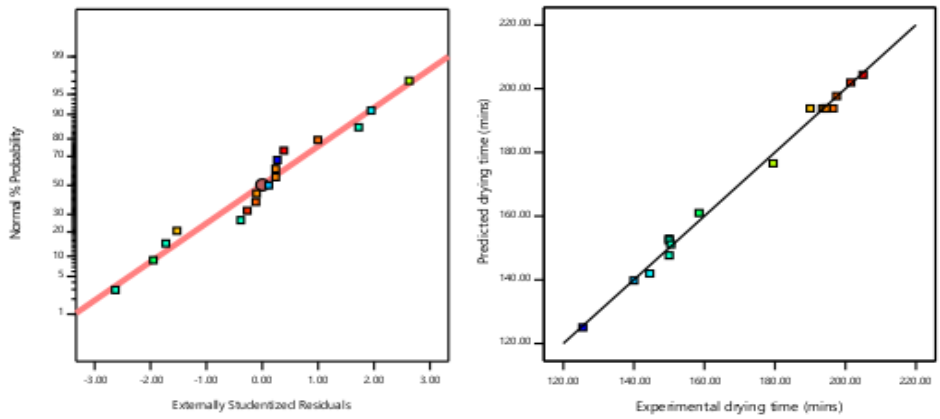

(a) **(b)**

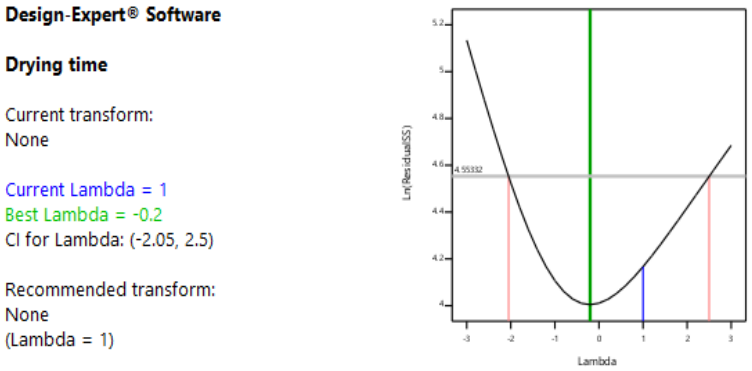

(c)

Figure 12. (a) Normal probability plot of drying time residuals; (b) Predicted versus experimental total energy consumption of red pepper; (c) Box-Cox plot for power transformation

Optimization Analysis

The affirmation of the optimal conditions of hybrid PV/T solar dryer was done using the multivariate response surface technique of Design Expert Statistical Software (version 11), with respect to Eq. (2). The desirability of the control variables (T, V and S) is unity, because their goal for numerical optimization (minimum energy consumption, maximum drying efficiency and minimum drying time and percent shrinkage of the dried products) is set "in range" as shown in Table 2. The optimization of response variables: E_t and η_d were at maximum level, whereas S_h and T_d were minimum. Different treatment combinations were obtained that satisfied the objective function and goals for the numerical optimization of this study. The optimal process conditions and response variables, as well as the overall desirability index are

presented in Table 5. It is evident that the model predicted the experimental values very closely at 95% confidence level, which yielded an overall desirability index of 0.899 for the control factors. A combined desirability at the optimum sample thickness (14.31 mm) is depicted in Fig. 13. The design points of the response factors were located on three distinct colour bands: blue, green, and red, designating the lower, average, and upper limits of the input parameters. The maximum desirability of 0.903 was obtained at 70°C and 1.88m/s drying air temperature and air velocity, respectively. This however, indicates that drying air temperature had a more noticeable influence in the optimization result of convective sir drying process of red pepper slices. The prediction accuracy of the RSM results was validated by conducting a drying experiment, with the values of the optimal input variables and the exact values of the response factors in Table 5 were obtained. Also, the percentage error of deviations of the predicted and experimental values, which are less than 5% were used to validate the models for E_t, η_d, S_h, and T_d (Aneke *et al.,* 2018). Thus, the obtained models adequately described the convective drying process of red pepper slices in a hybrid PV/T solar dryer.

Table 5. Optimal process conditions in the desirability range

Condition	T (°C)	V (m/s)	S (mm)	E_t (kWh)	η_d (%)	S_h (%)	T_d (mins)	Desirability index
Predicted				4.03	20.46	67.00	183.80	0.899
Optimum	70.0	1.88	14.31					0.903
Experimental				3.18	23.69	64.17	145.29	-
% Error	-	-	-	0.211	0.158	0.042	0.209	-

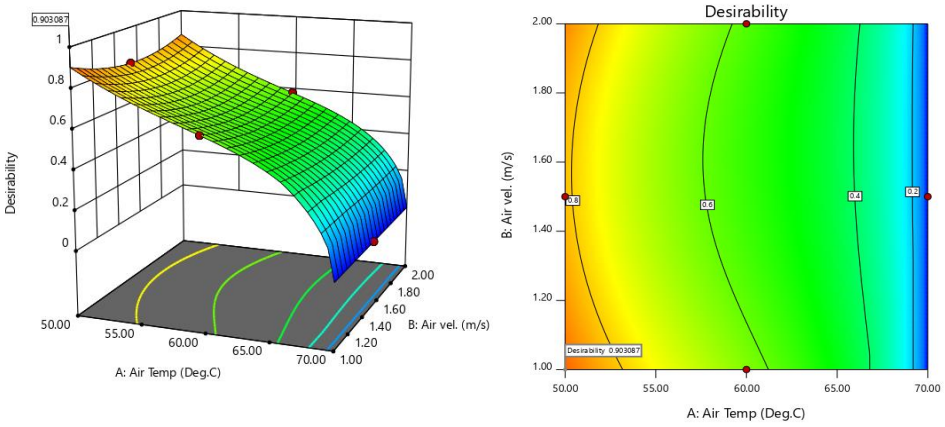

(a) **(b)**

Figure 13. Response surface plot of the combined desirability at optimum condition (a) 3-D surface plot, (b) 2-D contour plot

CONCLUSIONS

Sliced red pepper samples were convectively dried from initial to desired final moisture contents of 81.9 to 10%w.b, respectively using a hybrid photovoltaic-thermal solar dryer during rainy season in South-eastern Nigerian climate. The influence of varying drying variables on the total energy consumption, drying efficiency, percentage shrinkage and drying time were estimated using the desirability index of

the multivariate responses of numerical optimization of the drying process. The following conclusions can be made following the experimental findings of this study:

i. The thermal contribution of the solar cell and solar collector to the hybrid system drying energy varies between $0.792\% \leq Q_{pv} \leq 23.53\%$, and $0.518\% \leq Q_{col} \leq 15.37\%$, respectively.
ii. The total and specific energy consumption of red pepper slices varied between 1.31 – 38.9 kWh and 6.92 – 62.76 kW/kg, respectively; with the minimum energy obtained at 70°C drying air temperature, 2.0 m/s air velocity and 10 mm sample thickness, whereas the maximum values were obtained at 50°C drying air temperature, 1.0 m/s air velocity and 20 mm sample thickness.
iii. The mean drying efficiency of the system varied between 6.73 and 35.14%, whereas the percentage sample shrinkage ranged between $56.91\% \leq S_h \leq 73.90\%$.
iv. Minimum drying time occurred at 70°C drying air temperature, 1.5m/s air velocity and 10mm sample thickness. The drying time of red pepper ranges between $125.5 \pm 7 \leq T_d \leq 205.5 \pm 10$ mins.
v. The predicted optimum drying conditions of the sample were 70°C air temperature, 1.88 m/s air velocity and 14.31 mm sample thickness for maximum desirability of 0.994, the predicted response factors were 4.03kWh, 20.46%, 67.05% and 183.8 mins for total energy consumption, drying efficiency, shrinkage, and drying time, respectively.
vi. The quadratic models developed adequately predicted the experimental values very closely with an overall desirability index of 0.873 for the control factors and high R^2-values ranging between 0.9228 - 0.9989. Diagnostic plots and percentage error deviations were adopted for validation of model adequacy and prediction accuracy.

DECLARATION OF COMPETING INTEREST

The author(s) must declare that they have no conflict of interest.

CREDIT AUTHORSHIP CONTRIBUTION STATEMENT

The authors declared that the following contributions are correct.
Sampson Uzoma: Conceptualization, writing of original manuscript, data collation.
Nnaemeka Nwakuba: Writing of original manuscript draft, design of experiment, formal analysis, investigation, review and editing of manuscript.
Kelechi Anyaoha: Methodology, data analysis, validation, review and editing of manuscript.

ACKNOWLEDGMENT
Special thanks to TETFund Abuja and Imo State Polytechnic, Umagwo-Ohaji for providing the financial support for this research work. The technical and moral supports of the Works Unit of Imo State Polytechnic, Umagwo-Ohaji are sincerely appreciated.

REFERENCES

Abano EE, Ma H and Qu W (2014). Optimization of drying conditions for quality dried tomato slices using response surface methodology. *Journal of Food Process and Preservation, 38: 996-1009.*

Afolabi TJ, Akintunde TY and Oyelade OJ (2014). Influence of drying conditions on the effective moisture diffusivity and energy requirements of ginger slices. *Journal of Food Research, 3(5): 103-112.*

Ahmad WM, Zakaria SB, Aleng NA, Halim N. and Ali Z (2015). Box-Cox transformation and bootstrapping approach to one simple t-test. *World Applied Sciences Journal, 33 (5): 704-708.*

Anaeke NAG, Mbah GO and Edeani NJ (2018). Response surface methodology for optimization of ot air drying of water yam slices. *International Journal of Scientific and Research Publications, 8 (8): 248-259.*

Azadbakht M, Torshizi, VM Ziaratban, A and Aghili H (2017). Energy and exergy analysis during eggplant drying in a fluidized bed dryer: *Agricultural Engineering International, CIGR E-Journal. 19 (3): 177-82.*

Beigi M (2016). Energy efficiency and moisture diffusivity of apple slices during convective drying. *Food Science and Technology, 36 (1): 145-150.*

Boughali S, Benmoussa H, Bouchekima B, Mennouche D, BouguettaiaH. and Bechki D (2009). Crop drying by indirect active hybrid solar-electrical dryer in the eastern *Algerian Septentrional Sahara: Solar Energy, 83: 2223-2232.*

Corzo O, Bracho N, Vasquez A. and Pereira A (2008). Optimization of a thin layer drying process for coroba slices. *Journal of Food Engineering*, *85: 372-380.*

Darvishi H, Asi RA, Asghari A, Najafi G and Gazori HA (2013). Mathematical modeling, moisture diffusion, energy consumption and efficiency of thin-layer drying of potato slices: *Journal of Food Process Technology, 4 (3): 215-229.*

Dianda B, Ousmane M, Kam S, Ky Tand Bathiebo, DJ (2015). Experimental study of the kinetics and shrinkage of tomato slices in convective drying: *African Journal of Food Science, 9 (5): 262-271.*

Duffie JA and Beckman WA (2006). Solar Engineering of Thermal Process. *Wiley*, New York.

Erbay Z and Icier F (2009). Optimization of hot air drying of olive leaves using response surface methodology. *Journal of Food Engineering, 91: 533-541.*

Freedman D, Pisani R and Purves R (2007). Statistics 4th, *W.W Norton & CO*, New York, Pp. 20 -23.

Hafezi, N, Sheikhdavoodi, MJ and Sajadiye SM (2015). The effect of drying kinetic on shrinkage and colour of potato slices in the vacuum-infrared drying method. *International Journal of Agricultural and Food Research*, *4 (1): 24-31.*

Han QH, Yin LJ, Li SJ, Yang BN and Ma JW (2010). Optimization of process parameters for microwave vacuum drying of apple slices using response surface method. *Drying Technology, 28 (4): 523-532.*

Kumar D, Prasad S and Murthy GS (2011). Optimization of microwave-assisted hot air drying conditions of okra using response surface methodology. *Journal of Food Science and Technology, 4: 1-13.*

Lopez-Vidana EC, Mendez-Lagunas LL and Rodriguez-Ramirez J (2013). Efficiency of a hybrid solar-gas dryer. *Solar Energy, 93: 23-31.*

Minaei SA, Motevali D and Khoshtagaza MH (2011). Evaluation of energy consumption in different drying methods. *Energy Conversion and Management, 52 (2): 1192-1199.*

Minaei S, Chenarbon HA, Motevali A and Arabhosseini A (2014). Energy consumption, thermal utilization efficiency and hypericin content in drying leaves of St. John's Wort (*Hypericum Perforatum*): *Journal of Energy in Southern Africa, 25 (3): 27-35.*

Mortezapour H, Ghobadian B, Khostaghaza M. and Minaei S (2012). Performance analysis of a two-way hybrid photovoltaic/thermal solar collector. *Journal of Agricultural Science Technology*, *14: 767-780.*

Ndukwu MC, Simo-Tagne M, Abam FI, Onwuka OS, Prince S and Bennamoun L (2020a). Exergetic sustainability and economic analysis of hybrid solar-biomass dryer. *Heliyon, 6 (e03401):1-13.*

Ndukwu MC, Onyenwigwe D, Abam FI, Eke AB and Dirioha C (2020). Development of a low-cost wind-powered active solar dryer integrated with glycerol as thermal storage. *Renewable Energy, 154: 553-568*. https://doi.org/10.1016/j.renene.2020.03.016.

Nwakuba NR, Asoegwu SN and Nwaigwe KN (2016a). Energy requirements for drying of sliced agricultural products: a review. *Agricultural Engineering International. CIGR E-Journal, 18(2), 144-155.*

Nwakuba NR, Asoegwu SN and Nwaigwe KN (2016b). Energy consumption of agricultural dryers: an overview. *Agricultural Engineering International: CIGR Journal, 18 (4):119-132.*

Nwakuba NR, Chukwuezie OC, Asonye GU and Asoegwu SN (2018). Energy analysis and optimization of thin layer drying conditions of okra. *Arid Zone Journal of Engineering, Technology And Environment 14: 135-154.*

Nwakuba NR (2019). Optimization of energy consumption of a solar-electric dryer during hot air drying of tomato slices. *Journal of Agricultural Engineering, 50 (4): 150-158.*

Poonia S, Singh AK and Jain D (2018). Design development and performance evaluation of photovoltaic/thermal (PV/T) solar dryer for drying of ber (*Zizyphus mauritiana*) fruit. *Cogent Engineering, 5: 1-18.*

Reyes A, Mahn A, Huenulaf P and Gonzalez T (2014). Tomato dehydration in a hybrid solar dryer. *Chemical Engineering Processing Technology*, *5: 1-8.*

Sanusi MM and Ayinde IA (2013). Profitability of pepper production in derived savannah zone of Ogun State, Nigeria. *International Journal of Agriculture and Food Security 4 (1): 401-410.*

Sumic Z, Vakula A, Tepic A, Cakarevic J, Vitas J and Pavlic, B (2016). Modeling and optimization of red currants vacuum drying process by response surface methodology (RSM). *Food Chemistry, 203:465-475.*

Tiwari GN (2012). Solar energy fundamentals, design, modeling and application. *Narosa Publishing House PVT Ltd.*, New Delhi, pp. 203 – 250.

Uzoma S, Nwakuba NR and Anyaoha KE (2019). Performance of Hybrid Photovoltaic/Thermal Crop Dryer in Hot Humid Nigerian Region. *Journal of Agricultural Engineering, 2(XLIV): 56-75.*